APS physics

CHORUS

This is the accepted manuscript made available via CHORUS. The article has been published as:

# New method of analytic continuation of elastic-scattering data to the negative-energy region, and asymptotic normalization coefficients for ^{17}O and ^{13}C

L. D. Blokhintsev, A. S. Kadyrov, A. M. Mukhamedzhanov, and D. A. Savin

Phys. Rev. C **100**, 024627 — Published 28 August 2019

DOI: 10.1103/PhysRevC.100.024627

# New method of analytic continuation of elastic-scattering data to the negative-energy region and asymptotic normalization coefficients for $^{17}$O and $^{13}$C

L. D. Blokhintsev,[1] A. S. Kadyrov,[2] A. M. Mukhamedzhanov,[3] and D. A. Savin[1]

[1] *Skobeltsyn Institute of Nuclear Physics, Lomonosov Moscow State University, Moscow 119991, Russia*
[2] *Curtin Institute for Computation and Department of Physics and Astronomy, Curtin University, GPO Box U1987, Perth, WA 6845, Australia*
[3] *Cyclotron Institute, Texas A&M University, College Station, Texas 77843, USA*

A new method is proposed for extrapolation of elastic-scattering data to the negative-energy region for a short-range interaction. The method is based on the analytic approximation of the modulus-squared of the partial-wave scattering amplitude and can serve as an alternative to the traditional one based on continuation of the effective-range function. The new method has been applied to determine the asymptotic normalization coefficients for the $^{17}$O and $^{13}$C nuclei in the $n$+$^{16}$O and $n$+$^{12}$C channels, respectively. The asymptotic normalization coefficients obtained by the new method are compared with the ones obtained in the effective-range function approach.

## I. INTRODUCTION

Neutron-induced processes and neutron transfer reactions play an important role in nuclear reactions, nuclear astrophysics, and applied physics. In recent years these reactions have attracted a great interest due to their role in primordial nucleosynthesis of light elements [1] and in inhomogeneous Big Bang models where $(n, \gamma)$ processes take part in reaction chains leading to the synthesis of heavy elements [2, 3]. While the elements lighter than iron are either created during the Big Bang or fusion reactions in stars, most of the elements heavier than iron are produced via neutron-induced reactions [1]. Therefore, the knowledge of neutron-capture cross sections for stable and unstable isotopes is essential. In many cases low-energy neutron radiative-capture reactions and neutron-transfer reactions populate loosely-bound states of final nuclei. To calculate the cross sections of such reactions one needs to know full information about the final bound states, in particular, their quantum numbers, binding energies, and asymptotic normalization coefficients (ANCs).

Using scattering data may give valuable information on ANCs, which, in contrast to binding energies, cannot be directly measured. The ANCs are fundamental nuclear characteristics that are important, for example, for evaluating cross sections of peripheral astrophysical nuclear reactions [4–7]. One of the direct ways of extracting ANCs from experimental data is the analytic continuation in the energy plane of the partial-wave elastic-scattering amplitudes, obtained by the phase-shift analysis, to the pole corresponding to a bound state. Such a procedure, in contrast to the method of constructing optical potentials fitted to scattering data, allows one to circumvent an ambiguity problem associated with the existence of phase-equivalent potentials [8, 9].

The conventional procedure for such extrapolation is the analytic approximation of the experimental values of the effective-range function (ERF) $K_l(E)$ with the subsequent continuation to the pole position ($l$ and $E$ are the orbital angular momentum and the relative kinetic energy of colliding particles, respectively). The ERF method has been successfully employed to determine the ANCs for bound (as well as resonant) nuclear states in a number of works (see, e.g. [10–12] and references therein).

In our previous works [13–15] we investigated analytical continuation of scattering data for charged particles to the negative-energy region to obtain information about ANCs. In the present paper, a new method is proposed for extrapolating data on elastic scattering of neutrons. When analyzing neutron scattering, in contrast to scattering of charged particles, one deals only with a short-range interaction. The method developed here makes use of the modulus-squared, denoted as $M_l(E)$, of the partial-wave scattering amplitude $f_l(E)$. Since $M_l(E)$ is a real analytic function of $E$ on the real positive semi-axis of $E$ including $E = 0$, it can be analytically approximated by polynomials in $E$ for $E > 0$ and then analytically continued to the bound state pole to obtain information on the ANC. The method is based on the well-known and reliably established fact that the partial-wave amplitude of elastic scattering has a pole of the first order in energy at the point corresponding to the bound state, and the residue at this point is expressed in terms of the square of the ANC.

Within an exactly solvable model, it is shown that the proposed method has an advantage over the traditional one based on the continuation of the ERF. Using the available data on phase shifts, two versions of the new method, along with the ERF method, have been applied to determine the ANCs for the $^{17}$O and $^{13}$C nuclei in the $n$+$^{16}$O and $n$+$^{12}$C channels, respectively.

Performing experiments on neutron elastic scattering is not an easy task. However, for heavier nuclei, where the Coulomb interaction significantly complicates extrapolation of the proton elastic-scattering phase shifts, progress in new experimental facilities and methods can make measurements of neutron elastic scattering a valuable technique to obtain information about neutron ANCs using the extrapolation method suggested in this paper. The method provides faster convergence than the tradi-

tional one based on ERF. This is a significant advantage especially when experimental data have bigger uncertainties. In addition, using the mirror symmetry one can determine the proton ANCs from the extracted neutron ANCs.

The paper is organized as follows. In Sec. II, the theoretical backgrounds of the proposed method are outlined. Sections III and IV deal with the $n$+$^{16}$O and $n$+$^{12}$C systems, respectively.

Throughout the paper we use the system of units in which $\hbar = c = 1$.

## II. NEW METHOD OF ANALYTIC CONTINUATION OF A PARTIAL-WAVE ELASTIC-SCATTERING AMPLITUDE

Consider the partial-wave amplitude of elastic two-particle scattering $f_l(E)$ for a short-range interaction ($l$ is the orbital angular momentum, $E = k^2/2\mu$ is the relative kinetic energy of colliding particles, $k$ is their relative momentum, $\mu$ is the reduced mass). Denote $E = E_+$ if $E > 0$ and $E = E_-$ if $E < 0$.

Suppose that in the system under consideration there is a bound state with energy $E = -\varepsilon = -\varkappa^2/2\mu < 0$. For $E > 0$, we have

$$f_l(E_+) = \frac{k^{2l}}{D_l(E_+)}, \quad f_l^*(E_+) = \frac{k^{2l}}{D_l^*(E_+)}, \tag{1}$$

$$D_l(E_+) = k^{2l+1}(\cot\delta_l - i). \tag{2}$$

Introduce a quantity $M_l(E)$ according to

$$M_l(E_+) \equiv |f_l(E_+)|^2 = \frac{k^{4l}}{N_l(E_+)}, \tag{3}$$

$$N_l(E_+) = k^{4l+2}(\cot^2\delta_l + 1). \tag{4}$$

Since

$$N_l(E) = K_l^2(E) + k^{4l+2}, \tag{5}$$

$$K_l(E) = k^{2l+1}\cot\delta_l, \tag{6}$$

and the effective-range function $K_l(E)$ can be expanded in a series in $k^2$ near $k = 0$, the function $N_l(E)$ can also be expanded in a series in $k^2$ (or in $E$) near $E = 0$. Therefore, one can approximate $N_l(E)$ with the expression

$$N_l(E) = (E + \varepsilon)F_l(E), \tag{7}$$

where $F_l(E)$ is a polynomial or a rational function of $E$. The function $N_l(E)$ as given by Eq. (7) can be analytically continued to the domain $E < 0$. The $E + \varepsilon$ factor provides the pole of the amplitude $f_l(E)$ at the energy corresponding to the bound state. When $E \to -\varepsilon$ we have

$$\lim_{E\to-\varepsilon}[(E+\varepsilon)M_l(E)] = \lim_{E\to-\varepsilon}\left[(E+\varepsilon)\frac{k^{4l}}{(E+\varepsilon)F_l(E)}\right] = \frac{\varkappa^{4l}}{F_l(-\varepsilon)}. \tag{8}$$

On the other hand, using the connection between the residue of $f_l(E)$ and the asymptotic normalization coefficient $C_l$ (see, for example, [13, 16]) and considering that as $E \to -\varepsilon$, $\cot\delta_l \to i$, we have

$$\lim_{E\to-\varepsilon}[(E+\varepsilon)f_l(E)] = -\frac{1}{2\mu}C_l^2, \tag{9}$$

$$\lim_{E\to-\varepsilon} f_l^*(E) = \lim_{E\to-\varepsilon}\frac{k^{2l}}{k^{2l+1}(\cot\delta_l + i)} = -\frac{1}{2\varkappa}. \tag{10}$$

Combining (9) and (10), we get

$$\lim_{E\to-\varepsilon}[(E+\varepsilon)M_l(E)] = \lim_{E\to-\varepsilon}[(E+\varepsilon)f_l(E)f_l^*(E)] = \frac{C_l^2}{4\mu\varkappa}. \tag{11}$$

Comparing (8) and (11) gives the final result

$$C_l^2 = \frac{4\mu\varkappa^{4l+1}}{F_l(-\varepsilon)}. \tag{12}$$

In this method, in contrast to the method based on the continuation of the ERF $K_l(E)$, when defining the ANC $C_l$, there is no need to use the procedure of differentiation, impairing the accuracy of the results.

Consider a slightly different version of the approximation of $M_l(E)$ for $E > 0$:

$$M_l(E) = |f_l(E)|^2 = |e^{i\delta_l}\sin\delta_l/k|^2 = \sin^2\delta_l/k^2. \tag{13}$$

Note that $\delta_l$ is an odd function of $k$ and $\sin^2\delta_l$ is an even function of $k$. Therefore, taking into account the threshold behavior of $\delta_l$, one can write:

$$M_l(E) = \frac{k^{4l}}{E+\varepsilon}G_l(E), \tag{14}$$

where $G_l(E)$ is a polynomial or a rational function of $E$. From here, taking into account (11), we obtain:

$$\lim_{E\to-\varepsilon}[(E+\varepsilon)M_l(E)] = \varkappa^{4l}G_l(-\varepsilon) = \frac{C_l^2}{4\mu\varkappa} \tag{15}$$

and

$$C_l^2 = 4\mu\varkappa^{4l+1}G_l(-\varepsilon). \tag{16}$$

The expression (16) differs from (12) only by replacing $1/F_l(E)$ with $G_l(E)$.

Unfortunately, it is not clear how to generalize this method to include the Coulomb interaction since the renormalized Coulomb-nuclear partial-wave amplitude $\tilde{f}_l^*(E)$, unlike $\tilde{f}_l(E)$, has an essential singularity on the physical sheet of $E$ at $E = 0$ and is complex at $E < 0$ [13, 14].

## III. $n$+$^{16}$O SYSTEM

In this section, we consider the $n$+$^{16}$O system in the $J^\pi = 1/2^+$ state, since only for this state data on the phase-shift analysis are available in the literature. By continuing these data to a point corresponding to the bound state energy $E = -\varepsilon_1$ we determine the ANC $C_0$ for the excited state of the nucleus $^{17}$O($1/2^+$; 0.8707 MeV) in the $n$+$^{16}$O (ground state) channel. Various continuation methods are compared: the continuation of the ERF $K_0(E)$ and the continuation of the functions $F_0(E)$ and $G_0(E)$ introduced in Section II. Note that the determination of the ANC for the mirror nucleus $^{17}$F in the $p$+$^{16}$O channel by extrapolating the elastic-scattering data was carried out in [15].

The following mass values are used in the calculations: $m_{^{17}\mathrm{O}} = 15830.501$ MeV, $m_{^{16}\mathrm{O}} = 14895.079$ MeV, and $m_n = 939.565$ MeV.

### A. Theoretical $n$+$^{16}$O phase shifts

In this subsection, theoretical phase shifts $\delta_0$ calculated for the square-well potential from [17] are used to compare different ways of continuing the scattering data to the negative-energy region. The parameters of the potential are: $V_0 = 35.14$ MeV, $R = 4.21$ fm. This potential leads to two bound $s$-states, the lower of which is forbidden. The upper (allowed) state corresponds to the values of the binding energy $\varepsilon_1 = 3.59515$ MeV and ANC $C_0 = 2.83896$ fm$^{-1/2}$. Note that a more accurate experimental value of the binding energy is $\varepsilon_1 = 3.27227$ MeV.

This paper uses a more traditional deviation estimate based on the method of least squares [18],

$$\chi^2 = \frac{1}{N_p - N_f} \sum_{i=1}^{N_p} \left[ \frac{F(E_i) - f(E_i)}{\epsilon_i} \right]^2, \qquad (17)$$

where $N_p$ is the number of points, and $N_f$ is the number of parameters of the approximating function, $\epsilon_i$ is the error of the approximated function. Equation (17) takes into account the number of degrees of freedom and has several advantages over the definition used in the previous work [15]. This paper uses the approximation of continued functions by polynomials in energy $E$. For a polynomial of degree $N$, $N_p - N_f = N_p - N - 1$.

For theoretical phase shifts, the errors of the approximated functions are assumed to be equal to each other (for simplicity, $\epsilon_i = 1$ for all $i$). We start with the continuation of the ERF $K_0(E)$. While continuing $K_0(E)$ in all calculations in this work, a point corresponding to the energy of a bound state $E = -\varepsilon$ is added to points where phase shifts are known.

The results of the continuation are presented in Table I. As one can see, for large degrees of the approximating polynomial, a breakdown occurs due to the excess of accuracy, and the approximation becomes very different from the approximated function. It can be seen that the visible breakdown occurs at $N = 11$. The best ANC value according to the $\chi^2$ criterion corresponds to $N = 9$ and is equal to $C_0 = 2.84815$ fm $^{-1/2}$, that is, the deviation from the exact value is about 0.3 %. Dashes in the tables indicate the absence of a bound state with the correct theoretical energy.

TABLE I: ANC obtained by approximating ERF $K_0(E)$ for the $n$+$^{16}$O, $J^\pi = 1/2^+$ state using a polynomial of degree $N$.

| $N$ | $C_0$, fm$^{-1/2}$ | $\chi^2$ |
|---|---|---|
| 1 | - | $0.360438\times10^{-3}$ |
| 2 | 2.06155 | $0.204316\times10^{-5}$ |
| 3 | 5.33880 | $0.104794\times10^{-7}$ |
| 4 | 2.73289 | $0.382649\times10^{-10}$ |
| 5 | 3.08486 | $0.916381\times10^{-13}$ |
| 6 | 2.74633 | $0.221163\times10^{-15}$ |
| 7 | 2.88457 | $0.811685\times10^{-18}$ |
| 8 | 2.81882 | $0.130191\times10^{-19}$ |
| 9 | 2.84815 | $0.143192\times10^{-20}$ |
| 10 | 2.83505 | $0.666668\times10^{-20}$ |
| 11 | - | $0.153103\times10^{-15}$ |
| exact | 2.83896 | |

We now consider the continuation of the function $G_0(E)$ introduced in Eq. (14). The results of the continuation are presented in Fig. 1 and in Table II. The best result is achieved again with $N = 9$. As we can see the ANC at $N = 9$ reproduces the exact ANC to six significant digits.

TABLE II: ANC obtained by approximating function $G_0(E)$ for the $n$+$^{16}$O, $J^\pi = 1/2^+$ state using a polynomial of degree $N$.

| $N$ | $C_0$, fm$^{-1/2}$ | $\chi^2$ |
|---|---|---|
| 1 | 2.50251 | $0.278856\times10^{-4}$ |
| 2 | 2.79892 | $0.204894\times10^{-7}$ |
| 3 | 2.84871 | $0.255913\times10^{-11}$ |
| 4 | 2.84452 | $0.285314\times10^{-13}$ |
| 5 | 2.84042 | $0.270672\times10^{-16}$ |
| 6 | 2.83926 | $0.197367\times10^{-19}$ |
| 7 | 2.83902 | $0.743249\times10^{-23}$ |
| 8 | 2.83897 | $0.217671\times10^{-26}$ |
| 9 | 2.83896 | $0.548333\times10^{-28}$ |
| 10 | 2.83897 | $0.668000\times10^{-28}$ |
| exact | 2.83896 | |

Finally, we consider the continuation of the function $F_0(E)$ introduced in Eq. (7). The results of the extrapolation are presented in Table III. The best result

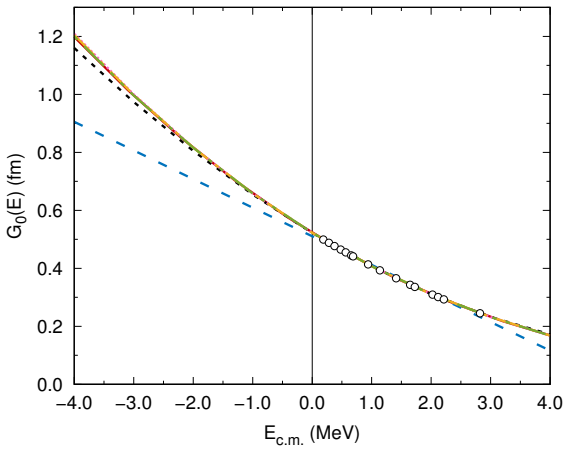


FIG. 1: Function $G_0(E)$ for $n$+$^{16}$O, $J^\pi = 1/2^+$. Solid red line represents the results obtained from the theoretical phase shifts, long-dashed blue line - the 1st-order polynomial, short-dashed black line - the 2nd-order polynomial, dotted pink line - the 3rd-order polynomial, dash-dotted yellow line - the 4th-order polynomial, dash-double-dotted green line - the 5th-order polynomial. Starting from the 3rd-order polynomial, the results are indistinguishable from the solid red line.

corresponds to $N = 12$ and the relative error of the ANC at $N = 12$ with respect to the exact ANC is $1.5 \times 10^{-4}$.

TABLE III: ANC obtained by approximating function $F_0(E)$ for the $n$+$^{16}$O, $J^\pi = 1/2^+$ state using a polynomial of degree $N$.

| $N$ | $C_0$, fm$^{-1/2}$ | $\chi^2$ |
|---|---|---|
| 1 | - | $0.652168\times10^{-2}$ |
| 2 | 1.73852 | $0.826223\times10^{-4}$ |
| 3 | - | $0.542466\times10^{-6}$ |
| 4 | 2.22777 | $0.205841\times10^{-8}$ |
| 5 | 3.48689 | $0.695829\times10^{-11}$ |
| 6 | 2.61596 | $0.333772\times10^{-13}$ |
| 7 | 2.98402 | $0.989157\times10^{-16}$ |
| 8 | 2.77309 | $0.250929\times10^{-18}$ |
| 9 | 2.87203 | $0.753178\times10^{-21}$ |
| 10 | 2.82183 | $0.293600\times10^{-23}$ |
| 11 | 2.84813 | $0.380000\times10^{-26}$ |
| 12 | 2.83852 | $0.183333\times10^{-26}$ |
| 13 | 2.85509 | $0.150000\times10^{-26}$ |
| 14 | 2.62132 | $0.220000\times10^{-26}$ |
| exact | 2.83896 | |

Comparison of the data from Tables I-III reveals that the fastest convergence with increasing degree $N$ of the approximating polynomial and the highest accuracy of the results for ANC $C_0$ occur in the case of approximation of the function $G_0(E)$. In fact, in this case a good level of convergence is achieved already at $N = 3$.

### B. Experimental $n$+$^{16}$O phase shifts

In this subsection, we use 16 values of phase shifts $\delta_0$ from [17, 19, 20], which correspond to the following neutron energy values $E_n$ in the laboratory system: $E_n$ = [0.20, 0.30, 0.40, 0.51, 0.60, 0.698, 0.73, 1.00, 1.21, 1.50, 1.75, 1.833, 2.15, 2.250, 2.353, 3.000] MeV.

For illustration, we also use the theoretical square-well potential with the parameters $V_0 = 34.90941226$ MeV, $R$ = 4.191822098 fm. This potential is close to the potential used in subsection III A. For the upper (allowed) $s$-state of $^{17}$O, it leads to the correct experimental binding energy $\varepsilon_1 = 3.27227$ MeV and ANC $C_0 = 2.6$ fm$^{-1/2}$. As in subsection III A, we compare the results of the extrapolation of the functions $K_0(E)$, $G_0(E)$, and $F_0(E)$.

Experimental and theoretical phase shifts for the $n$ + $^{16}$O system in the $J^\pi = 1/2^+$ state are depicted in Fig. 2. We see that the above potential describes the experimental data quite well.

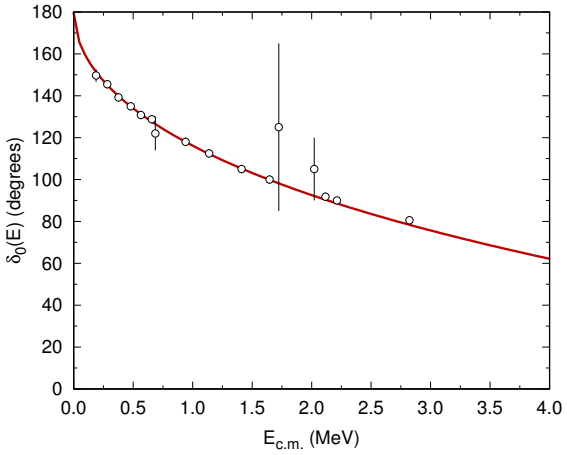


FIG. 2: Experimental and theoretical phase shifts for $n$ + $^{16}$O, $J^\pi = 1/2^+$. The experimental points are from [17, 19, 20]. The theoretical results are obtained using the square-well potential described in the text.

The results of the extrapolation of ERF $K_0(E)$ are presented in Fig. 3. As can be seen from this figure, for large degrees of the approximating polynomial, a breakdown occurs, and the approximation becomes very different from the approximated function. The best variant according to the $\chi^2$ criterion is $N = 2$ and leads to $C_0 = 2.20716$ fm$^{-1/2}$. In case of continuing $G_0(E)$ (see Fig. 4), the best ANC value by the $\chi^2$ criterion is $C_0$ = 2.67254 fm$^{-1/2}$, which, as in the case of ERF continuation, corresponds to $N = 2$. When extrapolating the $F_0(E)$ function (Fig. 5), again, the $N = 2$ variant is best by the $\chi^2$ criterion leading to $C_0 = 1.80667$ fm$^{-1/2}$.

We see that different ways of continuing the experimental data lead to slightly different results for the ANC

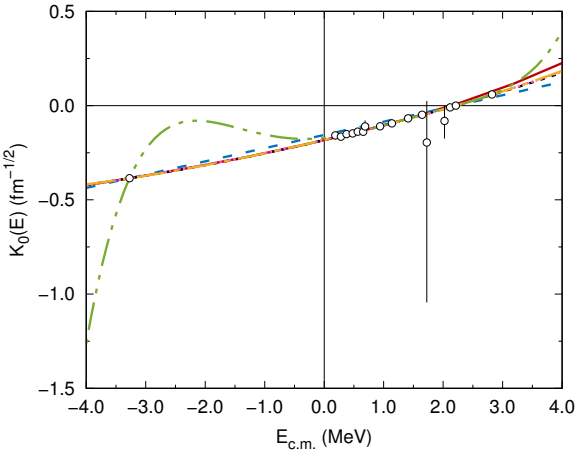


FIG. 3: ERF for $n$+$^{16}$O, $J^\pi = 1/2^+$. Solid red line represents the results obtained from theoretical phase shifts, long-dashed blue line - the 1st-order polynomial, short-dashed black line - the 2nd-order polynomial, dotted pink line - the 3rd-order polynomial, dash-dotted yellow line - the 4th-order polynomial, dash-double-dotted green line - the 5th-order polynomial. Starting from the 3rd-order polynomial, the results are indistinguishable. Points represent the results obtained from the experimental phase shifts.

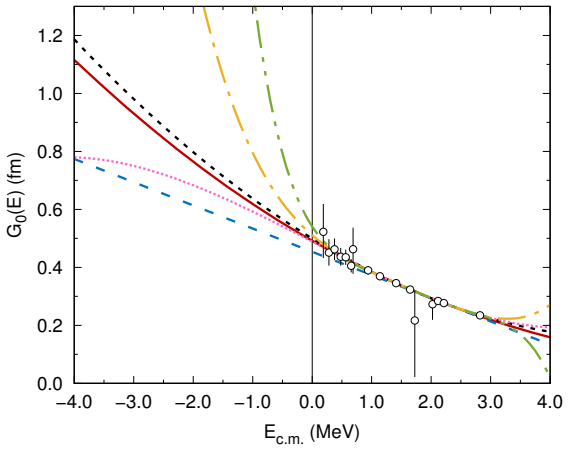


FIG. 4: The same as in Fig. 3 but for function $G_0(E)$.

$C_0$. This may be due to the low accuracy of the phase shift analysis used. The mean value of $C_0$, corresponding to the above three values, is $C_0 = 2.23 \pm 0.30$ fm$^{-1/2}$.

## IV. $n$+$^{12}$C SYSTEM

This section discusses the $n$+$^{12}$C system in the $1/2^+$ state for which phase-shift data are available. By continuing the scattering data to a point corresponding to the experimental energy of the bound state $E = -\varepsilon_2 = 1.856557$ MeV, the ANC $C_0$ is determined for the excited state of the nucleus $^{13}$C($1/2^+$; 3.089 MeV) in the

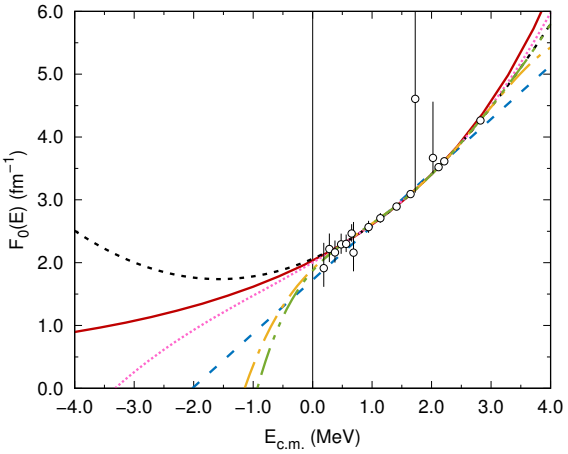


FIG. 5: The same as in Fig. 3 but for function $F_0(E)$.

channel $n$+$^{12}$C(ground state). As in Section III, the results obtained by extrapolating functions $K_0(E)$, $F_0(E)$, and $G_0(E)$ are compared. The following mass values are used: $m_{^{13}\mathrm{C}} = 12109.481$ MeV, $m_{^{12}\mathrm{C}} = 11174.862$ MeV, and $m_n = 939.565$ MeV.

### A. Theoretical phase shifts $n$+$^{12}$C

In this subsection, the theoretical phase shifts $\delta_0$, calculated for the square-well potential with the parameters $V_0 = 35.6753320221032$ MeV and $R = 4.02818653449678$ fm, are used to compare the effectiveness of various continuation methods. This potential leads to two bound $s$-states of $^{13}$C, the lower of which is forbidden. The upper (allowed) state corresponds to the experimental value of the binding energy $\varepsilon_2 = 1.856557$ MeV and ANC $C_0 = 1.60$ fm$^{-1/2}$.

For theoretical phase-shift values, the errors of the approximated functions are assumed to be equal to each other (for simplicity, $\epsilon_i = 1$ for all $i$).

The results of the continuation of the functions $K_0(E)$, $G_0(E)$, and $F_0(E)$ are presented in Tables IV, V and VI. For all continuation versions, the best ANC values $C_0$ by the $\chi^2$ criterion are close to the exact result. Comparing Tables IV-VI we conclude that, as in the case of the $n$+$^{16}$O system, the fastest convergence with increasing degree $N$ of the approximating polynomial and the highest accuracy of the results for ANC $C_0$ takes place in the case of extrapolating the function $G_0(E)$. The results of the continuation of the function $G_0(E)$ are shown in Fig. 6.

### B. Experimental $n$+$^{12}$C phase shifts

We use 16 neutron-energy points (laboratory system) from [21]: $E_n$ = [0.050, 0.100, 0.157, 0.207, 0.257, 0.307,

TABLE IV: ANC obtained by approximating ERF $K_0(E)$ for the $n$+$^{12}$C, $J^\pi = 1/2^+$ state using a polynomial of degree $N$.

| $N$ | $C_0$, fm$^{-1/2}$ | $\chi^2$ |
|---|---|---|
| 1 | 2.28097 | $0.867724\times10^{-5}$ |
| 2 | 1.52384 | $0.448646\times10^{-8}$ |
| 3 | 1.60788 | $0.434737\times10^{-10}$ |
| 4 | 1.11353 | $0.411513\times10^{-8}$ |
| 5 | 0.157698 | $0.431582\times10^{-6}$ |
| exact | 1.60 | |

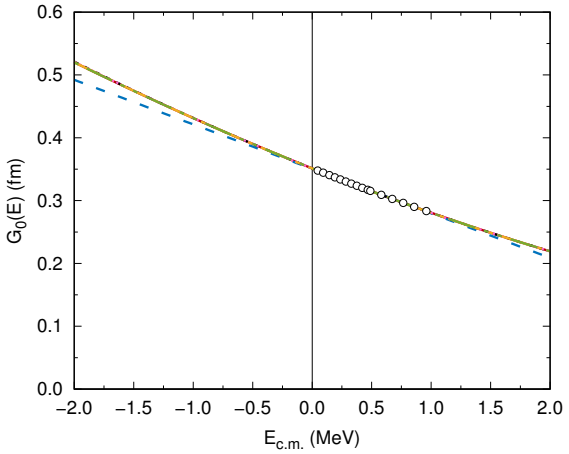


FIG. 6: Function $G_0(E)$ for $n$+$^{12}$C, $J^\pi = 1/2^+$. Solid red line represents the results obtained from theoretical phase shifts, long-dashed blue line - the 1st-order polynomial, short-dashed black line - the 2nd-order polynomial, dotted pink line - the 3rd-order polynomial, dash-dotted yellow line - the 4th-order polynomial, dash-double-dotted green line - the 5th-order polynomial. Starting from the 2nd-order polynomial, the results are indistinguishable.

0.357, 0.407, 0.457, 0.507, 0.530, 0.630, 0.730, 0.830, 0.930, 1.040] MeV.

Phase-shift errors are assumed to be $\pm1^\circ$. Note that increasing errors to $\pm2^\circ$ only leads to negligible changes in the results.

Experimental and theoretical phase shifts for the $n+{}^{12}$C system in the $J^\pi = 1/2^+$ state are depicted in Fig. 7. Theoretical phase shifts are calculated using the potential described in Subsection IV A. As in the case of the $n+{}^{16}$O system, there is good agreement between theory and experiment.

The results of the continuing the ERF $K_0(E)$ are presented in Fig. 8. The best ANC value by the $\chi^2$ criterion corresponds to $N = 1$ and is equal to $C_0 = 2.14638$ fm$^{-1/2}$. With the continuation of the function $G_0(E)$ (Fig. 9), the best ANC value is $C_0 = 1.87563$ fm$^{-1/2}$, corresponding to $N = 2$. Extrapolating the function $F_0(E)$ (Fig. 10) leads to the best value of $C_0 = 2.19107$ fm$^{-1/2}$, corresponding to $N = 1$. The mean value of $C_0$, corresponding to the above three values, is $C_0 = 2.07 \pm 0.13$ fm$^{-1/2}$.

TABLE V: ANC obtained by approximating function $G_0(E)$ for the $n$+$^{12}$C, $J^\pi = 1/2^+$ state using a polynomial of degree $N$.

| $N$ | $C_0$, fm$^{-1/2}$ | $\chi^2$ |
|---|---|---|
| 1 | 1.56036 | $0.125628\times10^{-6}$ |
| 2 | 1.60147 | $0.131839\times10^{-12}$ |
| 3 | 1.60109 | $0.816387\times10^{-14}$ |
| 4 | 1.60018 | $0.243129\times10^{-17}$ |
| 5 | 1.60002 | $0.330466\times10^{-21}$ |
| 6 | 1.60000 | $0.263367\times10^{-25}$ |
| 7 | 1.60000 | $0.513375\times10^{-27}$ |
| 8 | 1.60000 | $0.132814\times10^{-26}$ |
| 9 | 1.60002 | $0.213933\times10^{-26}$ |
| 10 | 1.59955 | $0.286980\times10^{-26}$ |
| exact | 1.60 | |

TABLE VI: ANC obtained by approximating function $F_0(E)$ for the $n$+$^{12}$C, $J^\pi = 1/2^+$ state using a polynomial of degree $N$.

| $N$ | $C_0$, fm$^{-1/2}$ | $\chi^2$ |
|---|---|---|
| 1 | 1.83289 | $0.708967\times10^{-4}$ |
| 2 | 1.54553 | $0.700486\times10^{-7}$ |
| 3 | 1.61637 | $0.616769\times10^{-10}$ |
| 4 | 1.59590 | $0.386920\times10^{-13}$ |
| 5 | 1.60102 | $0.238136\times10^{-16}$ |
| 6 | 1.59976 | $0.111939\times10^{-19}$ |
| 7 | 1.60006 | $0.548256\times10^{-23}$ |
| 8 | 1.59999 | $0.119700\times10^{-24}$ |
| 9 | 1.59990 | $0.213267\times10^{-24}$ |
| 10 | 1.60057 | $0.298720\times10^{-24}$ |
| exact | 1.60 | |

## V. CONNECTION BETWEEN MIRROR NEUTRON AND PROTON ANCS

In this section we discuss the possibility of obtaining the ANC for charged particles based on the ANC for uncharged particles (and vice versa). The ANC is the amplitude of the tail of the overlap function. While for neutrons the spherical Hankel function determines the radial shape of the tail, for protons the radial shape of the tail is determined by the Whittaker function. Nevertheless, the ratio of the proton and neutron ANCs of mirror state is practically model independent. The calculated proton and neutron ANCs themselves depend strongly on the

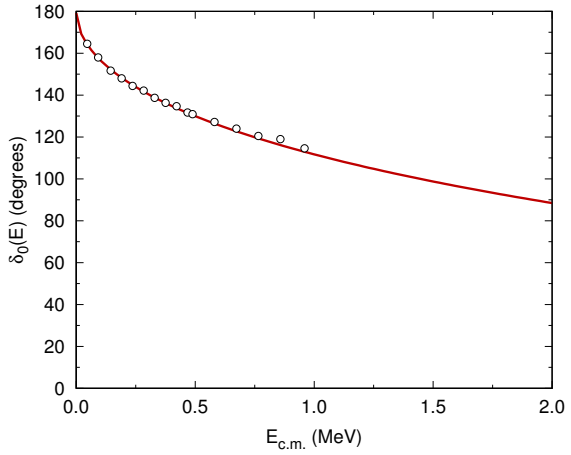


FIG. 7: Experimental and theoretical phase shifts for $n$+$^{12}$C, $J^\pi = 1/2^+$. The experimental points are from [21]. The theoretical results are obtained using the square-well potential described in the text.

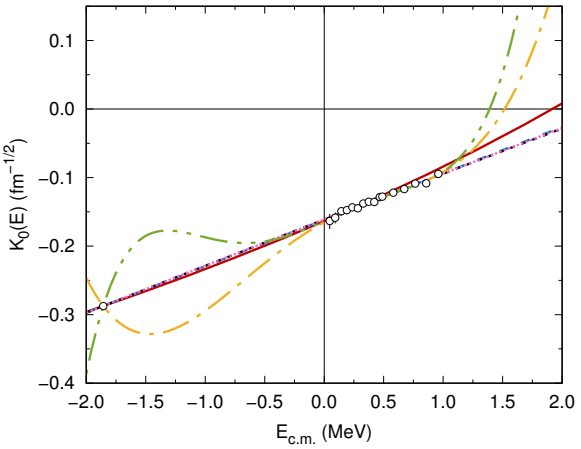


FIG. 8: ERF for $n$+$^{12}$C, $J^\pi = 1/2^+$. Solid red line represents the results obtained from theoretical phase shifts, long-dashed blue line - the 1st-order polynomial, short-dashed black line - the 2nd-order polynomial, dotted pink line - the 3rd-order polynomial, dash-dotted yellow line - the 4th-order polynomial, dash-double-dotted green line - the 5th-order polynomial. Points represent the results obtained from the experimental phase shifts.

choice of the nucleon-nucleon (NN) force but their ratios for mirror pairs should not depend on the choice of the NN force. This observation is based thus far entirely on the calculations using detailed models of nuclear structure. It follows naturally as a consequence of the charge symmetry of nuclear forces. Mirror nuclei have the same quantum numbers of mirror states.

The ratio of the proton and neutron ANCs is given by

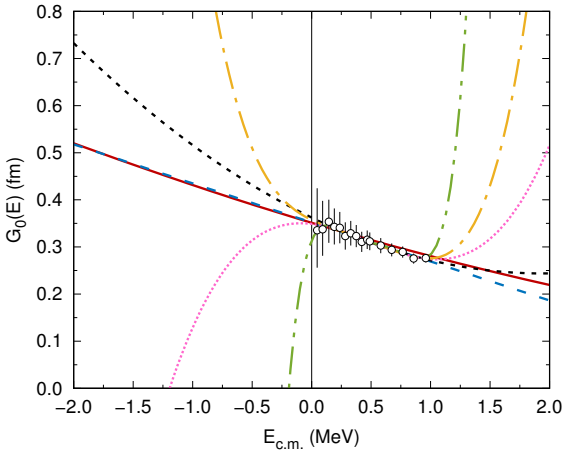


FIG. 9: The same as in Fig. 8 but for function $G_0(E)$.

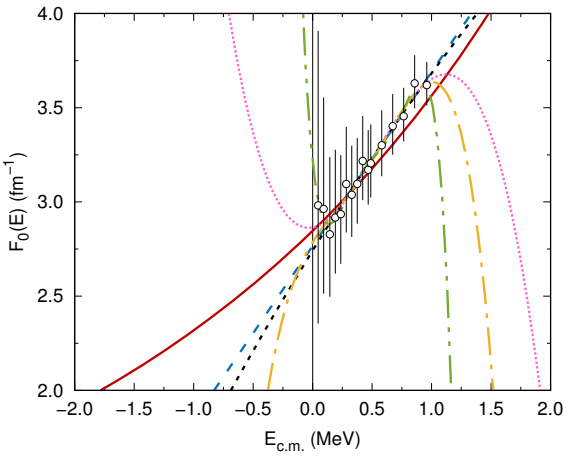


FIG. 10: The same as in Fig. 8 but for function $F_0(E)$.

[25]

$$\frac{C_p}{C_n} = \left| \frac{W[r_{pA}\, I^B_{pA}(r_{pA}),\, F_l(i\,\kappa_p,\, r_{pA})]|_{r_{pA}=R_{ch}}}{\kappa_p\, W[r_{nA}\, I^{A+1}_{nA}(r_{nA}),\, r_{nA}\, j_l(i\,\kappa_{nA}\, r_{nA})]|_{r_{nA}=R_{ch}}} \right|. \quad (18)$$

Here, $C_n \equiv C_0$ is the neutron ANC of the bound state $A+1 = (n\,A)$ and $C_p$ is the proton ANC of the mirror bound state $B = (p\,A)$, $I^{A+1}_{nA}$ ($I^B_{pA}$) is the radial overlap function of the bound-state wave functions of nuclei $A+1$ and $A$ ($B$ and $A$); $j_l(i\,\kappa_{nA}\,R_{ch})$ is the spherical Bessel function in the partial wave $l$ calculated at the imaginary momentum $i\,\kappa_{nA}$, $\kappa_{nA}$ is the bound-state-wave number of the mirror bound state $(n\,A)$; $e^{i\,\sigma^C_l}\, F_l(i\,\kappa_{pA},\, r_{pA})$ is the $p-A$ Coulomb regular solution in the partial wave $l$ calculated at the imaginary momentum $i\,\kappa_{pA}$, $\kappa_{pA}$ is the bound-state wave number of the bound state $(pA)$, $\sigma^C_l$ is the partial Coulomb scattering phase shift; $R_{ch}$ is the

$N-A$ nuclear interaction radius, which is assumed to be the same in both mirror states; $W[f,g]$ is the Wronskian of the function $f$ and $g$.

The Coulomb potential varies little over the nuclear volume and can be replaced by a constant equal to the difference between the neutron and proton binding energies. Hence, in the nuclear interior, which is all that matters on the right-hand side of Eq. (18), we can use [24, 25]

$$e^{i\,\sigma^C_{l_B}}\,F_{l_B}(i\,\kappa_{pA}\,r_{pA}) \approx \frac{e^{i\,\sigma^C_{l_B}}\,F_{l_B}(i\,\kappa_{pA},\,R_{ch})}{R_{ch}\,j_{l_B}(i\,\kappa_{nA}\,R_{ch})} \times r_{pA}\,j_{l_B}(i\,\kappa_{nA}\,r_{pA}). \qquad (19)$$

Taking into account that the mirror nucleon overlap functions are similar in the nuclear interior we can neglect their difference in Eq. (18). Then, in view of Eq. (19), we get the ratio of the proton and neutron ANCs of the mirror bound states:

$$\frac{C_p}{C_n} \approx \left|\frac{e^{i\,\sigma^C_l}\,F_l(i\,\kappa_{pA},\,R_{ch})}{\kappa_{pA}\,R_{ch}\,j_l(i\,\kappa_{nA}\,R_{ch})}\right|. \qquad (20)$$

Thus, despite the fact that in the external region the behavior of the proton and neutron overlap functions is different, we can determine the ratio of the mirror proton and neutron ANCs in a model-independent way calculating the ratio of the internal scattering wave functions given by Eq. (20). From this ratio one can determine the proton ANC if the neutron experimental ANC is known.

Using Eq. (20) and the mean value of the neutron ANC $2.23 \pm 0.30$ fm$^{-1/2}$ for the $^{17}$O($\frac{1}{2}^+$) state obtained in Subsection III B we get the mirror ANC $68.0 \pm 21.0$ fm$^{-1/2}$. Taking into account the low accuracy of the experimental neutron phase shifts the obtained proton ANC is in a reasonable agreement with the proton ANC for $^{17}$F($\frac{1}{2}^+$) of $81 \pm 8.0$ fm$^{-1/2}$ reported in [26]. Note that if we use the neutron ANC value of 2.67 fm$^{-1/2}$ then the mirror proton ANC would be 81.9 fm$^{-1/2}$, in the perfect agreement with that from [26].

We draw attention of the reader on the huge difference between the neutron and proton ANC [25]. To understand this difference we can rewrite Eq. (20) as

$$\frac{C_p}{C_n} \approx \mathcal{R}_1\,\mathcal{R}_2\,\mathcal{R}_3, \qquad (21)$$

where the first factor

$$\mathcal{R}_1 = \frac{\Gamma(l+1+\eta)}{\Gamma(l+1)} \qquad (22)$$

is the major Coulomb renormalization factor [25, 27]. Here $\eta$ is the Coulomb parameter of the $(pA)$ bound state. In the case under consideration $\mathcal{R}_1 = 17.4$.

The second factor $\mathcal{R}_2$ takes into account the difference between the neutron binding energy 3.27 MeV and the proton binding energy 0.105 MeV. The binding energy of the neutron analogue state is larger than the corresponding proton binding energy (the Hamiltonian of the Schrödinger equation for the mirror proton state contains additional repulsive Coulomb interaction potential, which decreases the proton binding energy). $\mathcal{R}_2$ is given by

$$\mathcal{R}_2 = \frac{j_l(i\,\kappa_{pA}\,R_{ch})}{j_l(i\,\kappa_{nA}\,R_{ch})}. \qquad (23)$$

It can be obtained by replacing the Coulomb regular solution $e^{i\,\sigma^C_l}\,F_l(i\,\kappa_{pA},\,R_{ch})$ in Eq. (20) with $\kappa_{pA}\,R_{ch}\,j_l(i\,\kappa_{pA}\,R_{ch})$ taken at the proton bound-state wave number $\kappa_{pA}$. In the case under consideration $\mathcal{R}_2 = 0.64$.

The third factor affecting the proton ANC takes into account the final Coulomb effects which are left after removing the first two factors and is given by

$$\mathcal{R}_3 = \frac{\tilde{F}_l(i\,\kappa_{pA},\,R_{ch})}{\kappa_{pA}\,R_{ch}\,j_l(i\,\kappa_{pA}\,R_{ch})}. \qquad (24)$$

To obtain this factor one can replace $e^{i\,\sigma^C_l}\,F_l(i\,\kappa_{pA},\,R_{ch})$ in Eq. (20) with $\tilde{F}_l(i\,\kappa_{pA},\,R_{ch}) = e^{i\,\sigma^C_l}\,F_l(i\,\kappa_{pA},\,R_{ch})/\mathcal{R}_1$ and in the denominator the neutron bound-state wave number $\kappa_{nA}$ with the proton one $\kappa_{pA}$. For the case under consideration $\mathcal{R}_3 = 2.73$.

Then we can write that the Coulomb ANC is $C_p = 17.4 \times 0.63 \times 2.73 \times C_n = 30\,C_n$. It is important to underscore that all these estimations do not require the knowledge of the mirror proton and neutron bound state wave functions. All we need is the Coulomb regular solution and the spherical Bessel functions.

It is worth noting that due the additional Coulomb interaction the proton mirror state can be a resonance. In this case the neutron ANC allows one to determine the resonance width of the mirror proton state. For more detailed discussion, see [23].

## VI. CONCLUSIONS

In the present paper, we proposed a new method of extrapolating elastic scattering data to the negative energy region for a short-range interaction. The method is based on the well-known and reliably established fact that the partial-wave amplitude of elastic scattering has a pole of the first order in energy at the point corresponding to the bound state, and the residue at this point is expressed in terms of the square of the ANC. The developed method, being an alternative to the traditional ERF one, provides an independent method of extrapolation of the elastic scattering data to the bound-state poles to determine the neutron ANCs. Taking into account the low accuracy of the neutron elastic scattering phase shifts, application of two independent extrapolation techniques will provide more reliable information about the neutron ANCs. Moreover, we demonstrate that using

the mirror symmetry one can determine from the neutron ANC the mirror proton ANC. This connection is especially important for heavier nuclei where the measurements of the low-energy Coulomb-modified nuclear phase shifts to determine the proton ANC is practically impossible. We demonstrated here how one can determine the proton ANC for $^{17}\mathrm{F}(\frac{1}{2}^+)$ using the mirror neutron ANCs $^{17}\mathrm{O}(\frac{1}{2}^+)$ determined by three different extrapolation techniques. Moreover, if the mirror proton ANC is well established, one can determine the mirror neutron ANC. It will allow one to determine which extrapolation method has an advantage for a case under consideration. For example, for the case considered in this paper, the method based on extrapolation of function $F_0$ gave too low neutron ANC. On the other hand, using the neutron ANC value based on extrapolation of function $G_0$, the results are in the perfect agreement with the mirror proton ANC from [26].

Using the available phase-shift data, two versions of the new method, as well as the ERF method, have been applied to determine the ANCs for the excited $s$ states of $^{17}$O and $^{13}$C nuclei in the $n$+$^{16}$O and $n$+$^{12}$C channels, respectively. Due to the low accuracy of the phase-shift analysis used different ways of continuing the experimental data lead to slightly different results for the ANCs. The mean values of the ANCs obtained with all different methods used in this paper are $2.23\pm0.30$ fm$^{-1/2}$ for $^{17}$O and $2.07\pm0.13$ fm$^{-1/2}$ for $^{13}$C. For comparison, the ANC values obtained from the analysis of data on radiative neutron capture are 3.01 fm$^{-1/2}$ for $^{17}$O and 1.61 fm$^{-1/2}$ for $^{13}$ C [22]. These results are based on the assumption of the peripheral character of the $s$-wave radiative capture which is not justified. Therefore, the accuracy of these ANC values is difficult to estimate. On the other hand, the method proposed in this work is equally suitable for extrapolation of elastic scattering data for any $l$.

We emphasise that though the potential of a rectangular well form supporting two bound states is used in our work, the potential is not used to obtain any information about the real values of the ANC. For this purpose, we use the analytical continuation of experimental phase shifts. The potential model is used for methodological purposes since it allows one to accurately calculate the values of the ANC and phase shifts. Knowing these values, we establish which of the approximate methods of continuation of the scattering data to the negative-energy region allows us to better reproduce the exact theoretical values of the ANC. To achieve this goal, the number of bound states in the potential under consideration is irrelevant. We used the potential with two bound states simply because such a model better describes the properties of the actual systems under consideration and is commonly used in the literature. Although in principle, for our methodological purposes, one could use a potential with one bound state. The result does not depend on this choice.

**Acknowledgements**

This work was supported by the Russian Science Foundation Grant No. 16-12-10048 (L.D.B.) and the Russian Foundation for Basic Research Grant No. 18-02-00014 (D.A.S.). A.S.K. acknowledges a support from the Australian Research Council and the U.S. NSF Grant No. PHY-1415656. A.M.M. acknowledges support from the U.S. DOE Grant No. DE-FG02-93ER40773, the U.S. NSF Grant No. PHY-1415656, and the NNSA Grant No. DE-NA0003841.

[1] C. Rolfs and W. S. Rodney, *Cauldrons in the Cosmos* (Chicago, IL: University of Chicago Press, 1988).
[2] M. Heil et al., Astrophys. J. **507**, 997 (1998).
[3] Z. H. Liu *et al.*, Phys. Rev. **C 64**, 034312 (2001).
[4] A. M. Mukhamedzhanov and N. K. Timofeyuk, Yad. Fiz. (in Russian) **51**, 679 (1990) [Sov. J. Nucl. Phys. (English transl.) **51**, 431 (1990)].
[5] H. M. Xu, C. A. Gagliardi, R. E. Tribble, A. M. Mukhamedzhanov, and N. K. Timofeyuk, Phys. Rev. Lett. **73**, 2027 (1994).
[6] A. M. Mukhamedzhanov and R. E. Tribble, Phys. Rev. C **59**, 3418 (1999).
[7] R. E. Tribble, C. A. Bertulani, M. La Cognata, A. M. Mukhamedzhanov and C. Spitaleri, Rep. Prog. Phys. **77**, 106901 (2014).
[8] L. D. Blokhintsev and V. O. Eremenko, Phys. At. Nucl. **71**, 1219 (2008).
[9] Leonid Blokhintsev, Yuri Orlov, and Dmitri Savin, *Analytic and Diagram Methods in Nuclear Reaction Theory* (Nova Science Publishers, Inc., New York, 2017).
[10] L. D. Blokhintsev, V. I. Kukulin, A. A. Sakharuk, D. A. Savin, and E. V. Kuznetsova, Phys. Rev. C **48**, 2390 (1993).
[11] J.-M. Sparenberg, P. Capel, and D. Baye, Phys. Rev. C **81**, 011601 (2010).
[12] B. F. Irgaziev and Yu. V. Orlov, Phys. Rev. C **91**, 024002 (2015).
[13] L. D. Blokhintsev, A. S. Kadyrov, A. M. Mukhamedzhanov, D. A. Savin, Phys. Rev. C **95**, 044618 (2017).
[14] L. D. Blokhintsev, A. S. Kadyrov, A. M. Mukhamedzhanov, D. A. Savin, Phys. Rev. C **97**, 024602 (2018).
[15] L. D. Blokhintsev, A. S. Kadyrov, A. M. Mukhamedzhanov, D. A. Savin, Phys. Rev. C **98**, 064610 (2018).
[16] L. D. Blokhintsev, I. Borbely, and E. I. Dolinsky, Fiz. Elem. Chastits At. Yadra (in Russian) **8**, 1189 (1977) [Sov. J. Part. Nuclei (English transl.) **8**, 485 (1977)].
[17] J. L. Fowler, H. O. Cohn, Phys. Rev. **109** P. 89–93 (1958).
[18] J. Wolberg, *Data Analysis Using the Method of Least Squares. Extracting the Most Information from Experiments*, (Berlin; New York. Springer, 2006).
[19] J. L. Fowler, C. H. Johnson, Phys. Rev. C. **2**, 124–131 (1970).
[20] C. H. Johnson, J. L. Fowler, Phys. Rev. **162**, 890–899 (1967).

[21] S. B. Dubovichenko, *Phase-Shift Analysis in Nuclear Astrophysics* (LAP Lambert Academic Publishing, Saarbrücken, 2015), Section 2.3.4 (in Russian).
[22] J. T. Huang, C. A. Bertulani, and V. Guimarães, At. Data Nucl. Data Tables **96**, 824 (2010).
[23] A. M. Mukhamedzhanov, Phys. Rev. C **99**, 024311 (2019).
[24] N. K. Timofeyuk, R. C. Johnson, and A. M. Mukhamedzhanov, Phys. Rev. Lett. **91**, 232501 (2003).
[25] A. M. Mukhamedzhanov, Phys. Rev. C **86**, 044615 (2012).
[26] C. A. Gagliardi *et al.*, Phys Rev. C **59**, 1149 (1999).
[27] L. D. Blokhintsev, A.M. Mukhamedzhanov, and A. N. Safronov, Fiz. Elem. Chastits At., **15**, 1296 (1984) [Sov. J. Part. Nucl. (Engl. Transl.), **15**, 580 (1984)].